SIMULATION OF SEMICONDUCTOR DEVICES AND PROCESSES Vol. 5
Edited by S. Selberherr, H. Stippel, E. Strasser - September 1993

Simulation of Self-Heating Effects in a Power p-i-n Diode

K. Kells, S. Müller, G. Wachutka†, and W. Fichtner

Integrated Systems Laboratory, ETH-Zürich
Gloriastraße 35, CH-8092 Zürich, SWITZERLAND
†Quantum Electronics Laboratory, ETH-Zürich
ETH-Hönggerberg, CH-8093 Zürich, SWITZERLAND

Abstract

To accurately predict the effects of self-heating in a power p-i-n diode, we have applied self-consistent device simulation using a thermodynamically rigorous electrothermal model [1] implemented in the device/circuit simulator *Simul* [2]. Results of steady-state and high-voltage turn-off simulations with external electrical and thermal circuit elements are presented comparing the isothermal and self-heating cases.

1. Introduction

Two time frames are important when dealing with non-isothermal effects in the operation of semiconductor devices. Over longer times, a rise in lattice temperature due to self-heating can change mobility and intrinsic density in the bulk and/or channel of the device. On much shorter time scales, local hot spots may produce electrical currents and heat flow due to high temperature gradients. Extreme local heating can lead to local device breakdown, which can result in device failure.

Non-isothermal effects are included through the thermodynamic model in three ways. First, we introduce to the well-known current equations the gradient of the local lattice temperature T as an additional current driving force:

$$\vec{J}_n = -q\mu_n n(\nabla\phi_n + P_n\nabla T) \qquad \text{and} \qquad \vec{J}_p = -q\mu_p p(\nabla\phi_p + P_p\nabla T), \tag{1}$$

where P_n and P_p are the absolute thermoelectric powers. Since the quasi-Fermi potentials ϕ_n and ϕ_p also depend on temperature, $\nabla\phi_n$ and $\nabla\phi_p$ include temperature gradients which must not be neglected when extending the drift-diffusion model to non-isothermal conditions. Then, in addition to the Poisson and current continuity equations, we solve self-consistently the following time-dependent equation for the temperature:

$$c\frac{\partial T}{\partial t} = \nabla\cdot\kappa\nabla T + H \tag{2}$$

where κ is the thermal conductivity, c is the heat capacity, and H is the heat generation. Finally, the temperature dependence of the bulk parameters such as the intrinsic number, the mobility, and the thermoelectric powers is taken into account.

2. Dynamical equation and model considerations in *Simul*

The heating term H in Eqn. 2 is the full transient heat expression as given in [1] with the exception that the terms involving $\partial n/\partial t$ and $\partial p/\partial t$ are neglected as in [3], since estimations show that this term is negligible compared with the other heating terms up to $\partial n/\partial t$ or $\partial p/\partial t \approx 10^{21}\mathrm{cm}^{-3}\mathrm{s}^{-1}$. The upper bound of $\partial n/\partial t$ or $\partial p/\partial t$ in the p-i-n diode simulations was estimated to be $10^{14}\,\mathrm{cm}^{-3}\mathrm{s}^{-1}$.

Solution of the dynamical equations is carried out through decoupled iteration between the heat flow equation and the coupled system of electrical equations [4, 5].

The two most important temperature-dependent models in the p-i-n diode simulation are the effective intrinsic density and the mobility. Our mobility model takes into account doping dependence (μ_{doping}) and carrier-carrier scattering (μ_{cc}) combined using the Matthiessen rule [2]:

$$\mu_{\mathrm{doping}} = \mu_{\mathrm{min1}} \cdot \exp\left(\frac{-P_c}{N_i}\right) + \frac{\mu_L\,(T/300)^{-\zeta} - \mu_{\mathrm{min2}}}{1+(N_i/C_r)^{\alpha}} - \frac{\mu_1}{1+(C_s/N_i)^2} \tag{3}$$

$$\mu_{\mathrm{cc}} = \frac{D\,(T/300)^{3/2}}{\sqrt{(n\,p)}}\left[\ln\left(1+F(T/300)^2(pn)^{-1/3}\right)\right]^{-1} . \tag{4}$$

The dominating temperature effect is a decrease in mobility with rising temperature due to the explicit temperature dependence in Eqn. 3.

Our effective intrinsic density model is by default that of Slotboom [6]. In the steady state, we also investigated the models given in [7,

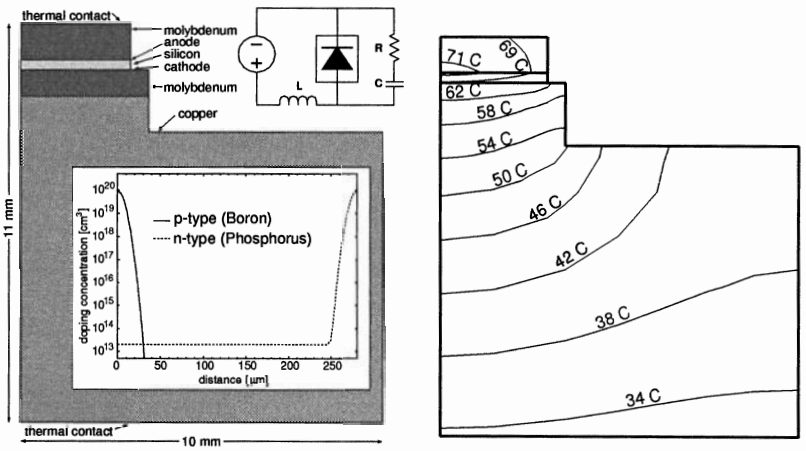

(a) (b)

Figure 1: p-i-n diode geometry, doping profile, and external circuit (a) and steady-state temperature distribution (b) in long-lifetime diode forward biased to $200\,\mathrm{A/cm}^2$.

3. Results and Discussion

The simulation device consists of a 280 μm thick and 3.0 mm wide silicon p-i-n diode sandwiched between two molybdenum plates and mounted on a copper heatsink. The simulation domain and the impurity concentration profile of the diode are shown in Fig. 1.a. Two

different carrier lifetimes are used for simulation; the "long-lifetime diode" has lifetimes $\tau_n = 28\,\mu s$ and $\tau_p = 9.33\,\mu s$, while the "short-lifetime diode" has lifetimes $\tau_n = 2.8\,\mu s$ and $\tau_p = 0.933\,\mu s$.

We assume that heat generated in the active area of the device flows to the surroundings through thermally resistive thermal contacts at the bottom of the heatsink ($R_{th} = 0.3\,K/W$) and along the top of the upper molybdenum plate ($R_{th} = 10\,K/W$) which are tied to $T = 300\,K$. Homogeneous Neumann boundary conditions (zero heat flux) are chosen for all other device surfaces.

The results of the steady-state simulation are shown in Fig. 2.a. At lower currents, the increase of the intrinsic density with temperature acts to increase current, while the decrease of the mobility with temperature dominates at higher currents and temperatures.

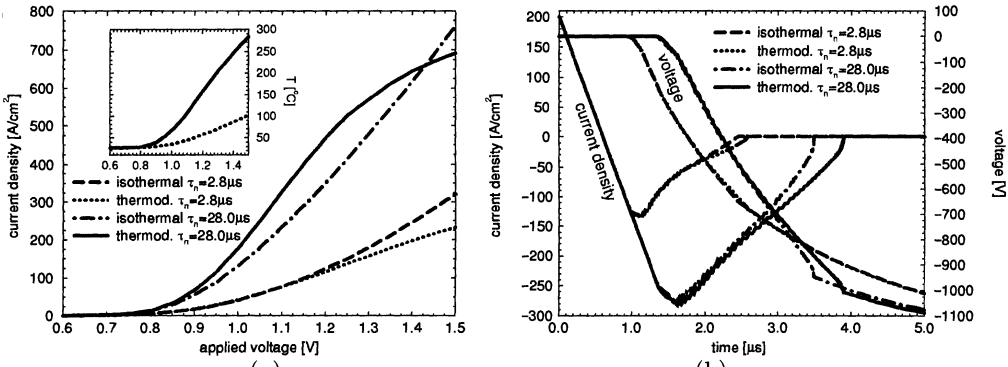

Figure 2: Steady-state current and maximum temperature vs. voltage (a) and comparison of isothermal and thermodynamic transient turn-off behavior (b) for both diodes.

For the transient simulation, both p-i-n diodes are turned off to a final blocking voltage of $-1\,kV$ from steady-state forward bias conditions of $200\,A/cm^2$. The electrical circuit used for the turn-off simulations is shown in Fig. 1.a. The values of R, L, and C for both diodes are $4.47\,\Omega$, $10\,\mu H$, and $2\,\mu F$, respectively, giving rise to a di/dt during turn-off of $-100\,A/\mu s$ using a total electrical contact area of $0.3\,cm^2$. The voltage supply switches linearly from the forward-bias voltage to $-1\,kV$ in $10\,ns$.

Fig. 2.b. shows the turn-off current as a function of time for both devices comparing the isothermal and thermodynamic case. The turn-off current in the thermodynamic simulations approaches zero more slowly than in the isothermal case, which is especially visible in the long-lifetime diode. This result agrees with the measured and simulated results published in [9].

The contributions of the individual heat generation mechanisms to the total heat in the long-lifetime diode integrated over the entire device are depicted in Fig. 3.a. In the initial state ($t = 0\,s$), the dominant heating mechanism is recombination heat at the p^+-i and i-n^+ junctions, in line with results presented in [10]. Another important term is the Peltier heat, which is also generated at the junctions. Since the sign of the Peltier heat is dependent on the direction of current flow, it is interesting to note that this heat is negative at $t = 0\,s$, but becomes positive during turn-off when the current reverses direction.

Joule heat generated by hole current is the dominating heating mechanism during turn-off, followed in importance by electron Joule heat and Peltier heat. After the diode has reached the blocking voltage, current due to impact ionization leads to small electron and hole Joule heat contributions. The current and consequently the Joule heating decrease

with decreasing device temperature, until the final thermal and electrical turn-off state is attained after approximately 5 seconds.

Shown in Fig. 3.b. is the temperature in the long-lifetime diode measured along the vertical axis along the left of the simulation domain for various times during the turn-off simulation. A temperature peak of about 85 °C is reached at about 4 μs into the turn-off simulation.

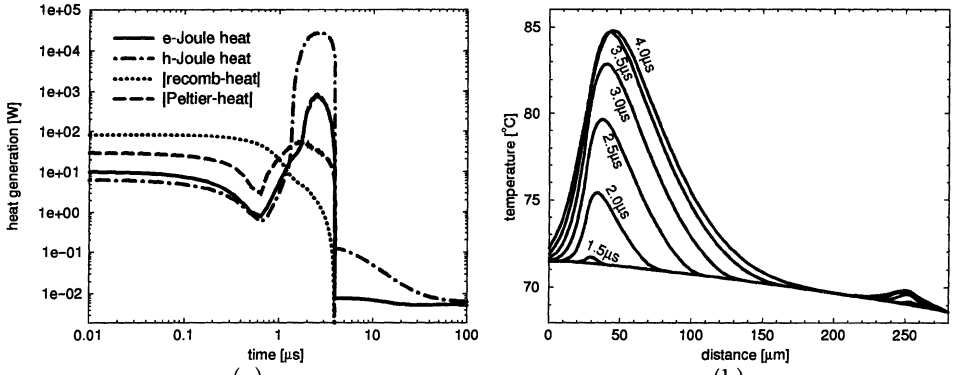

(a) (b)

Figure 3: Development of the various heating terms (a) with time during turn-off of the long-lifetime diode and lattice temperature (b) across the long-lifetime diode during turn-off.

References

[1] G. Wachutka, "Rigorous thermodynamic treatment of heat generation and conduction in semiconductor device modeling," *IEEE Trans.*, vol. CAD-9, pp. 1141–1149, 1990.

[2] IIS, *Simul Manual.* Integrated Systems Laboratory, ETH Zurich, Switzerland, 1.0 (alpha) ed., 1992.

[3] P. Wolbert, *Modeling and Simulation of Semiconductor Devices in TRENDY.* PhD thesis, University Twente, 1991. publ. by PROSA, P.O. Box 8091, 7550 KB Hengelo, Netherlands.

[4] V. Alwin, D. Navon, and L. Turgeon, "Time-dependent carrier flow in a transistor structure under nonisothermal conditions," *IEEE Trans. Elec. Dev.*, vol. ED-24, pp. 1297–1304, 1977.

[5] P. Gough, P. Walker, and K. Wright, "Electrothermal simulation of power semiconductor devices," in *Proc. ISPSD*, pp. 89–94, 1991.

[6] J. W. Slotboom and H. C. de Graaff, "Bandgap narrowing in silicon bipolar transistors," *IEEE Trans. Elec. Dev.*, vol. ED-24, no. 8, pp. 1123–25, 1977.

[7] J. del Alamo, S. Swirhun, and R. M. Swanson, "Measuring and modeling minority carrier transport in heavily doped Silicon," *Solid-State Electronics*, vol. 28, no. 1, pp. 47–54, 1985.

[8] D. B. M. Klaassen, J. W. Slotboom, and H. C. de Graaff, "Unified apparent bandgap narrowing in n- and p-type Silicon," *Solid-State Electronics*, vol. 35, no. 2, pp. 125–29, 1992.

[9] R. Kraus, T. Türkes, and H. Mattausch, "Modelling the self-heating of power devices," in *Proc. ISPSD*, pp. 124–129, 1992.

[10] D. Kakati, S. Ramanan, and V. Ramamurthy, "Computer-aided electrothermal analysis of a semiconductor device," in *Proc. of NASECODE IV Conf.*, pp. 326–331, 1985.